Remote Sensing of Environment 176 (2016) 272–281

Contents lists available at ScienceDirect

Remote Sensing of Environment

journal homepage: www.elsevier.com/locate/rse

Remotely sensed assessment of urbanization effects on vegetation phenology in China's 32 major cities

Decheng Zhou [a,b], Shuqing Zhao [b,*], Liangxia Zhang [a], Shuguang Liu [c]

[a] Jiangsu Key Laboratory of Agricultural Meteorology, and College of Applied Meteorology, Nanjing University of Information Science and Technology, Nanjing 210044, China
[b] College of Urban and Environmental Sciences, and Key Laboratory for Earth Surface Processes of the Ministry of Education, Peking University, Beijing 100871, China
[c] Geospatial Science Center of Excellence (GSCE), South Dakota State University, Brookings, SD 57007, United States

ARTICLE INFO

Article history:
Received 24 December 2014
Received in revised form 11 January 2016
Accepted 4 February 2016
Available online 13 February 2016

Keywords:
Start of growing season
End of growing season
Urban heat island
Vegetation phenology
Global warming
Urbanization

ABSTRACT

Urbanization-induced phenological shifts may provide evidence on how vegetation will respond to global warming. However, the effects of urbanization on vegetation phenology are poorly understood in urban environments. Using MODIS data between 2007 and 2013, we investigated the trends of the phenological metrics (i.e., start, end, and length of growing season: SOS, EOS and GSL) of individual cities and across cities relative to rural areas for China's 32 major cities. We found that the effects of urbanization on phenology decayed exponentially toward rural areas, and were closely related to the land surface temperature (LST) for more than half of the cities. The phenological sensitivity to temperature were 9–11 days SOS advance and 6–10 days EOS delay per 1 °C increase of LST. On average across all cities, the growing season started 11.9 days earlier and ended 5.4 days later in urban zones compared to rural counterparts. The urbanization effects increased with increasing latitudes, following the pattern of urban heat island effects in general. Our study suggests the value of urban environments in studying the phenological responses to future global change. However, the urbanization impacts are complex and need more direct observations, experimental manipulations, and cross-boundary inter-comparison studies.

© 2016 Elsevier Inc. All rights reserved.

1. Introduction

Change in vegetation phenology not only is a highly sensitive indicator of the effects of climate change but also can regulate climate by altering the energy, water, and carbon exchanges between land surface and the atmosphere (Baldocchi et al., 2001; Keenan et al., 2014; Piao et al., 2008; Richardson et al., 2010, 2013; Zhang, Friedl, & Schaaf, 2006). Numerous studies suggested that the vegetation phenology in the northern mid- to high-latitudes has been greatly altered by global warming, characterized by an earlier start and longer duration of growing season associated with increasing temperature (e.g., Aono & Kazui, 2008; Cong et al., 2012; Delbart et al., 2008; Dragoni & Rahman, 2012; Jeong, Ho, Gim, & Brown, 2011; Keenan et al., 2014; Piao, Fang, Zhou, Ciais, & Zhu, 2006; White et al., 2009; Zeng, Jia, & Epstein, 2011). However, both the magnitude, pattern, and mechanisms of the warming effects remain uncertain because of lacking long-term observations and the difficulties in manipulating field temperature for natural vegetation experimentally (Cong et al., 2012; Garonna et al., 2014; Jochner, Caffarra, & Menzel, 2013; Zeng et al., 2011).

Urban areas tend to have higher temperatures than the surroundings, referred to as urban heat island (UHI), largely resulted from the rise of impervious surface at the expense of vegetated and evaporating soil surfaces that reduces latent heat flux and increases sensible heat flux (Arnfield, 2003; Clinton & Gong, 2013; Oke, 1982). Cities with apparent UHI effects may provide a useful, unintended laboratory to assess how vegetation will respond to a global warming (Jochner et al., 2013; Luo, Sun, Ge, Xu, & Zheng, 2007; Mimet et al., 2009; Neil & Wu, 2006; White, Nemani, Thornton, & Running, 2002; Zhang, Friedl, Schaaf, Strahler, & Schneider, 2004; Ziska et al., 2003). For example, Zhang et al. (2004) reported that the phenological differences between urban and rural areas related linearly and significantly ($p < 0.0001$) to the temperature differences in the eastern North America, with 3 days advance of vegetation greenup for each 1 °C increase in temperature. The phenological shifts in urban areas can affect many ecological processes including net primary production (Imhoff et al., 2004) and seed set (Santandreu & Lloret, 1999). Phenological shifts may create an asynchronous mismatch between pollinators and their flowers (Kudo, Nishikawa, Kasagi, & Kosuge, 2004). In addition, prolonged growing season length (GSL) may affect human health by lengthening the allergy seasons and thus increasing the severity of allergies (Cecchi et al., 2010; van Vliet, Overeem, de Groot, Jacobs, & Spieksma, 2002). An accurate knowledge of the urbanization effect on phenology, therefore, can not only help enhance understanding the phenological responses to warming but also be essential for formulating mitigation strategies in cities.

* Corresponding author.
E-mail address: sqzhao@urban.pku.edu.cn (S. Zhao).

http://dx.doi.org/10.1016/j.rse.2016.02.010
0034-4257/© 2016 Elsevier Inc. All rights reserved.

At present, the effects of urbanization on vegetation phenology are poorly understood (Jochner, Sparks, Estrella, & Menzel, 2012; Jochner et al., 2013). First, whether there exists an urbanization effect remains inconclusive. Several studies observed advances of the start of growing season (SOS) and delays of the end of growing season (EOS) in urban areas relative to rural counterparts by field measurements (Lu, Yu, Liu, & Lee, 2006; Roetzer, Wittenzeller, Haechel, & Nekovar, 2000) or remote-sensing analyses (White et al., 2002; Zhang et al., 2004), whereas others demonstrated an insignificant change and even a delay of the SOS in urbanized areas for some cities (Gazal et al., 2008; Jochner et al., 2012, 2013). Second, the relationship between UHI and vegetation phenology is controversial. Zhang et al. (2004) indicated that the UHI intensities (urban–rural temperature differences) were significantly correlated with urban–rural phenological differences across cities, while other observations showed that UHI effects could not explain the urban–rural phenological differences for many cities especially in the tropical regions (Gazal et al., 2008) or for many species (Jochner et al., 2013). Third, the background climate was identified as one major driver for the large-scale spatial variability of vegetation activity (Piao et al., 2003), UHI intensity (Zhao, Lee, Smith, & Oleson, 2014; Zhou, Zhao, Liu, Zhang and Zhu, 2014), and the warming effect on vegetation (Cong et al., 2012), but its relationship with the phenological changes in urban areas is unclear. With accelerating urbanization (Angel, Parent, Civco, Blei, & Potere, 2011; Seto, Güneralp, & Hutyra, 2012; United Nations, 2014) and warming trend (IPCC, 2013) worldwide, there is a strong impetus to better understand the phenological shifts associated with urbanization over large areas.

As the world's most populous country, China experienced the rapidest urbanization in past decades in the world and the trend is expected to continue in upcoming decades (Seto, Fragkias, Güneralp, & Reilly, 2011; Seto et al., 2012; United Nations, 2014). Meanwhile, China covers a wide temperature gradient decreasing from south to north and a large precipitation gradient decreasing from southeast to northwest. Thus, China is ideal to examine the urbanization effect at a regional level. In this study, we analyzed the effect of urbanization on vegetation phenology in 32 major cities distributed across China using Moderate Resolution Imaging Spectoradiometer (MODIS) data in conjunction with cloud-free Landsat Thematic Mapper (TM) and Enhanced Thematic Mapper Plus (ETM+) images between 2007 and 2013. Our main objectives were to investigate (1) the trend of the urbanization effect on phenology of individual cities, (2) the spatial variability of the urbanization effects on phenology across cities, and (3) their relationship with UHI effects and background climate in China.

2. Data and methods

2.1. Remotely sensed vegetation phenology

Our study covered China's 32 major cities. They are municipalities or provincial capitals (mostly the largest city in the municipality or province) except Shenzhen, which is China's first special economic zone established in 1978 and is now considered as one of the global fastest growing cities (Fig. 1). Most cities are surrounded mainly by cultivated land, and the rest by forests (e.g., Hangzhou and Fuzhou) or grassland (Lhasa). Land cover maps within the administrative boundary of each city for the year 2010 were derived from the cloud-free Landsat TM/ETM+ images with a moderate spatial resolution of 30 m. The land covers were classified into four broad types (i.e., cropland, urban land, water body, and other land cover) using the maximum likelihood classification approach (Zhao et al., 2015). The accuracies of the classified products were assessed by using the high-resolution images and pictures incorporated in Google Earth Pro® (GE). The accuracies, measured by Kappa coefficients, were generally larger than 0.80 for all those cities. Further details on land cover data can be found in our

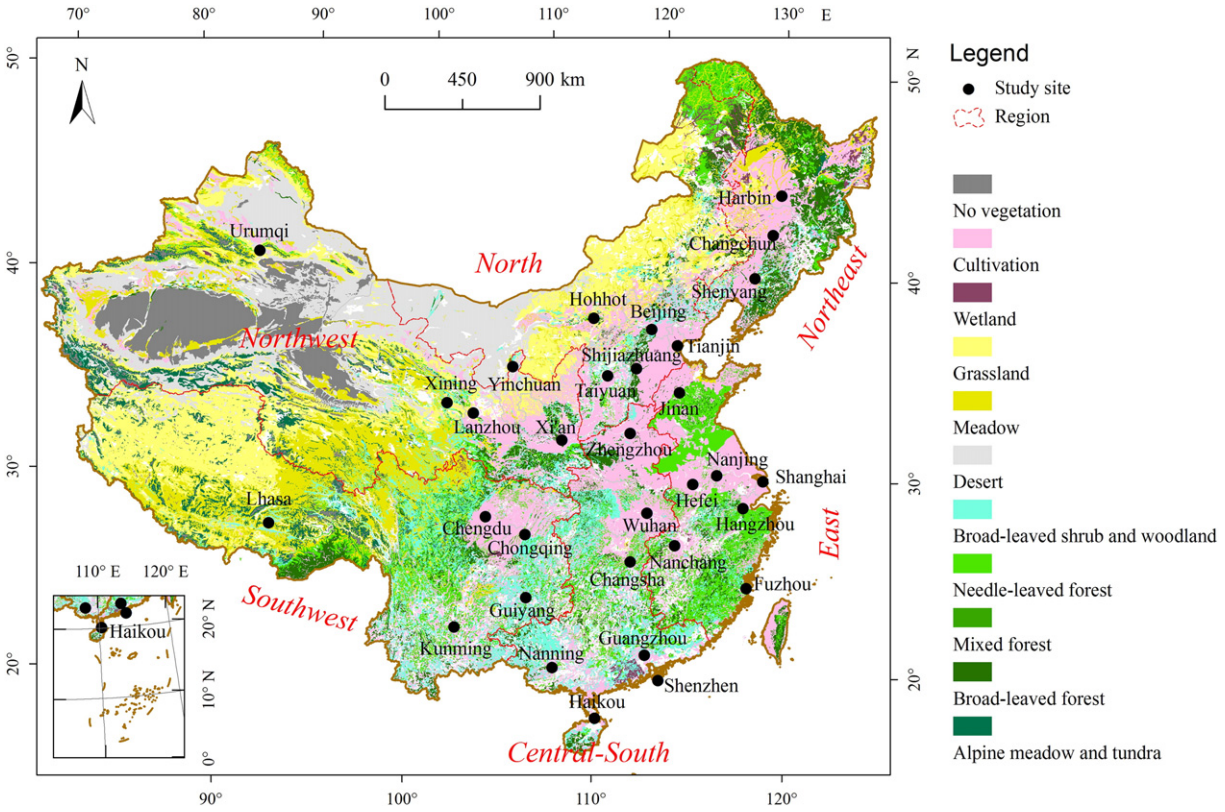

Fig. 1. Locations of the 32 major cities and six geographic regions in China, with the background indicating the vegetation map of China (this data set is provided by "Environmental & Ecological Science Data Center for West China, National Natural Science Foundation of China" (http://westdc.westgis.ac.cn)). All of the cities are municipalities or provincial capitals except Shenzhen, which is China's first special economic zone established in 1978, and is now considered one of the fastest-growing cities in the world. Albers Conical Equal Area was used as the projection coordinate system.

previous work (Zhao et al., 2015). To investigate the geographic variations of the urbanization effect on phenology, these cities were grouped into six geographic regions: North China (Beijing, Hohhot, Shijiazhuang, Taiyuan, and Tianjin), Northeast China (Changchun, Harbin, and Shenyang), East China (Fuzhou, Hangzhou, Hefei, Jinan, Nanchang, Nanjing, and Shanghai), Central-south China (Changsha, Guangzhou, Haikou, Nanning, Shenzhen, Wuhan, and Zhengzhou), Southwest China (Chengdu, Chongqing, Guiyang, Kunming, and Lhasa), and Northwest China (Lanzhou, Urumqi, Xi'an, Xining, and Yinchuan) (Fig. 1). The East, Central-south, and Southwest parts of China have typical humid-hot climate. Northeast China, North China, and Northwest China have typical humid cold, semi-humid/arid temperate, and arid climates, respectively.

The version-5 Aqua MODIS enhanced vegetation index (EVI, 16-day composite) with a spatial resolution of 250 m (MYD13Q1) was used to extract phenology information for the period 2007–2013. Compared with the most widely used normalized difference vegetation index (NDVI) (e.g., Jeong et al., 2011; Keenan et al., 2014; Piao et al., 2006; White et al., 2009; Zeng et al., 2011), the EVI minimizes the impacts of canopy background variations while retaining the sensitivity to small changes in vegetation activities (Dallimer et al., 2011), and its accuracy has been assessed over a widely range of locations and time periods (Huete et al., 2002). The EVI was believed to be more appropriate for monitoring vegetation dynamics in urban areas usually covered by sparse vegetation (Dallimer et al., 2011; Zhang et al., 2004; Zhou, Zhao, Liu and Zhang, 2014). The Aqua instead of Terra MODIS EVI datasets were used in order to keep accordance with the Aqua MODIS land surface temperature (LST) products used in this study, which were believed to be more representative for characterizing the UHI effects and thus being widely used in UHI studies (e.g., Clinton & Gong, 2013; Peng et al., 2012; Zhou, Zhao, Liu, Zhang and Zhu, 2014).

We focused on three phenological metrics in this analysis: SOS, EOS, and GSL, and the TIMESAT algorithms (Chen et al., 2004; Jönsson & Eklundh, 2004) were used to calculate these metrics based on EVI time series. Three methods were available in the TIMESAT software: adaptive Savitzky–Golay filtering, asymmetric Gaussian, and double logistic. Both asymmetric Gaussian and double logistic approaches use semi-local methods and can make good predictions of the SOS and EOS, especially for noisy time-series (Hird & McDermid, 2009). We applied the double logistic function since it performs better for data smoothing in high latitudes than the asymmetric Gaussian approach (Zeng et al., 2011).

Two methods were available to determine the dates of the SOS and EOS from EVI time series in TIMESAT software: a) start and end where fitted curve reaches a threshold value, and b) start and end where the fitted curve reaches a proportion of the seasonal amplitude measured from the left and right minimum values, respectively. The second method was utilized in this study because the EVI values in urban areas were usually much lower than that in buffer areas (Zhou, Zhao, Liu and Zhang, 2014), which make it difficult to find a threshold value to determine the SOS and EOS dates. We defined the SOS and EOS as 20% of the seasonal amplitude measured from the left and right minimum levels, respectively (Fig. 2). The proportion was selected based on the previous experiences (Brown, de Beurs, & Vrieling, 2010; Buyantuyev & Wu, 2012; Cong et al., 2012; Eklundh & Jönsson, 2009; White et al., 2009). The GSL was then estimated as the date differences between EOS and SOS.

We calculated the SOS, EOS, and GSL for each year separately during the period 2007–2013. Due to the complexity of urban surface, there were outliers for the phenological estimates. To reduce those uncertainties, pixels with the SOS earlier than the 50th day of year or later than the 180th day of year were excluded for the SOS analysis. The threshold values were loosely determined according to previous practices (Cong et al., 2012; White et al., 2009). Similarly, the EOS was constrained between the 240th and 330th day of year (Zhang et al., 2006). Following general practices in previous studies, we did not attempt to validate the remotely-sensed phenological metrics with field observations due to definition difference (i.e., ecosystem vs. species) and varying uncertainty sources (Rodriguez-Galiano, Dash, & Atkinson, 2015). Nevertheless, our approach for calculating phenological metrics is widely used in similar studies (e.g., Cong et al., 2012; Zeng et al., 2011) which has shown good agreement with ground observations in Europe (Rodriguez-Galiano et al., 2015).

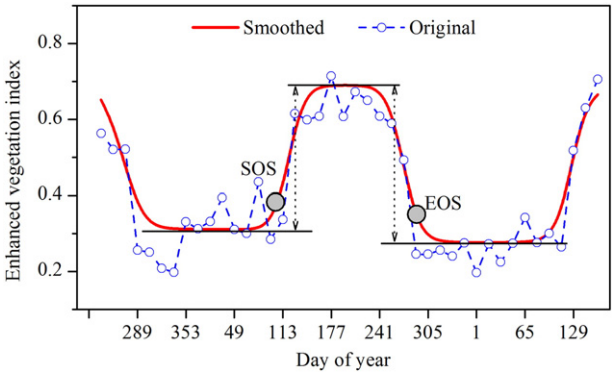

Fig. 2. Concept map shows the start of growing season (SOS) and the end of growing season (EOS) that were defined as 20% of the seasonal amplitude measured from the left and right minimum levels, respectively.

2.2. Identifying urbanization effect on phenology

We hypothesized that the effect of urbanization on phenology is strongest in urban centers and decreases gradually toward rural areas (e.g., Zhang et al., 2004). To demonstrate this effect, it is necessary to define and delineate urban and surrounding buffer areas on maps. The urban area was defined by three steps (Zhou, Zhao, Liu, Zhang and Zhu, 2014): 1) a built-up intensity (BI) map was generated from each urban coverage map using a 1 km × 1 km moving window method; 2) a 50% threshold of BI was used as a criterion to separate the BI maps into high- and low-intensity built-up land; and 3) the high-intensity built-up polygons were aggregated to delineate the urban border with an aggregation distance of 2 km, which is sufficient to include the scattered and most adjacent high-intensity built-up patches into the urban class. The urban areas ranged from 47.6 km^2 (Lhasa) to as much as 2350.6 km^2 (Tianjin) in the year 2010.

A series of buffers extending 0–1, 1–2, 2–5, 5–10, 10–15, 15–20, and 20–25 km from the urban edge outward were then created for all the 32 cities individually (Fig. 3A). In order to quantify the effect of urbanization on phenology, it is necessary to define the rural phenology (referring to the baseline or reference phenology) for each city. We defined the phenology in the farthest buffer (20–25 km) as rural or baseline reference. This definition should be able to reflect the background phenology because the mean footprint of urban areas on phenology had been estimated to be less than 20 km away from urban perimeter in eastern North America (Zhang et al., 2004) and China (Zhou, Zhao, Zhang, Sun, & Liu, 2015). Pixels that were water body or with elevation more than 50 m higher than the highest point in the urban area were excluded from this analysis because these pixels may overshadow the urbanization effects on phenology (e.g., White et al., 2002; Zhou, Zhao, Liu and Zhang, 2014). Digital Elevation Model (DEM) at a 3 arc-second (approximately 90 m) spatial resolution from the Space Shuttle Radar and Topography Mission (SRTM) (downloaded from http://earthexplorer.usgs.gov/) was used to exclude altitude effects.

We generated urban and buffer areas for each city in 2010 and assumed that the urban area and buffers delineated in 2010 can be used to represent those in 2007–2013. We did not remove cropland from this analysis as some previous efforts did (e.g., Buyantuyev & Wu, 2012; Zhang et al., 2004) for two main reasons. First, urbanization

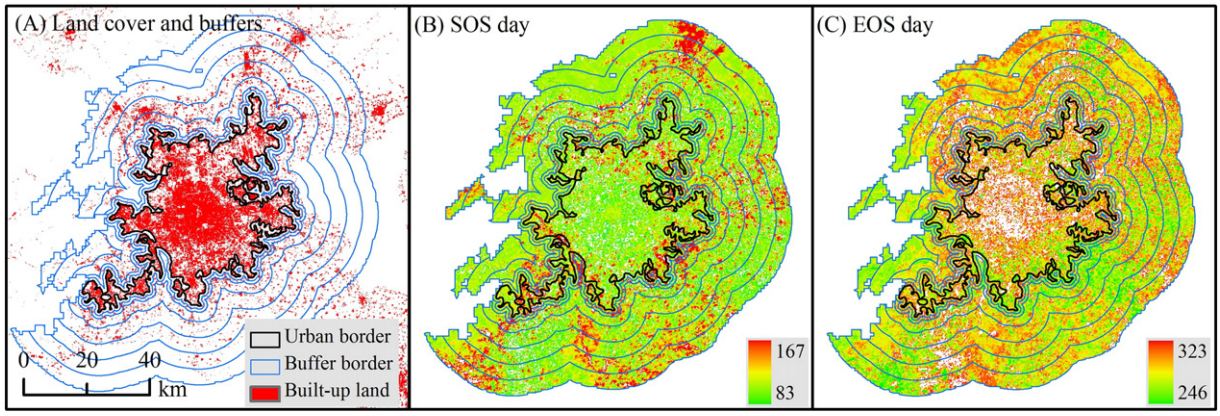

Fig. 3. The delineation of urban land cover, EOS day (day of year), EOS day (day of year), and seven buffer zones in the year 2010, an example of Beijing. Pixels that were water body or with elevation more than 50 m higher than the highest point in urban area were excluded from this analysis.

mainly occurred in agricultural land of China (Liu et al., 2005) and the resultant changes of phenology represent one essential part of the urbanization effect on vegetation. Second, the number of vegetated, non-agricultural pixels was too small for some cities to conduct reliable statistical analysis. For example, less than 10 EVI pixels were left after we removed the classified cropland in the 0–1 km and 1–2 km buffers in Xi'an, Shijiazhuang, and Hefei.

Then we calculated the phenological differences between urban or buffer zone and rural area for each city and each year separately as follow:

$$\Delta P = P_{ub} - P_r$$

where P_{ub} and P_r represent vegetation phenological metric (i.e., SOS, EOS, or GSL) in urban (or buffer) and reference rural areas, respectively. ΔP is their difference for a given phenological metric. A negative value of ΔP for SOS/EOS indicates an advance of the SOS/EOS, while the opposite means a delay. A positive value of ΔP for GSL demonstrates a prolonged growing season and vice versa. The phenological estimates may vary substantially by year due to climate variability, urban development, and/or varying data quality, we thus averaged the ΔP over the period 2007–2013 in order to capture the overall urban–rural phenological trend for each city.

2.3. Analysis

The trends of the SOS and EOS differences (relative to unaffected rural area, hereafter) from urban to rural areas were examined using an exponential decay model of individual cities based on previous findings (Zhang et al., 2004; Zhou et al., 2015). For the cities with significant decline trends ($p < 0.05$), we further explored their relationship with temperature differences across urban and buffer zones. The version-5 LST data from Aqua MODIS (MYD11A2, 8-day composite, and 1 km spatial resolution), monitored at 1:30 (nighttime) and 13:30 (daytime) local solar time, was used in this study. The LST was retrieved from clear-sky (99% confidence) observations using a generalized split-window algorithm (Wan & Dozier, 1996). It has been widely validated with the bias generally less than 1 K (Wan, 2008) in most cases and the mean absolute differences (relative to the in-situ measurements) less than 5% in urban areas (Rigo, Parlow, & Oesch, 2006). We calculated the LST differences using the same method as that for phenology. Since the SOS and EOS are mainly controlled by spring and autumn temperatures, respectively (Kramer, 1994), the correlations between the SOS/EOS differences and spring (March to May)/autumn (September to November) LST differences were analyzed using SPSS (SPSS Inc.).

To investigate the spatial variability of the urbanization effects on phenology across cities in China, we estimated the urban–rural differences of the SOS, EOS, and GSL in all six regions of China. To address the uncertainty introduced by the relatively small number of cities in each region, a nonparametric resampling procedure was used to generate bias-corrected bootstrap 95% confidence intervals of the phenological differences from 1000 randomizations of the observed phenological differences within each region in SPSS PASW Statistics 18 (SPSS Inc.). Significance tests ($p = 0.05$) were then conducted to determine (1) if the estimated phenological difference was statistically different from zero for each region (i.e., does the urbanization effect exist?), and (2) if there were differences in phenology across regions.

The relationship between spring/autumn urban–rural LST differences (refers to the UHI intensities) and urban–rural SOS/EOS differences were examined by general linear regression model. We also explored the climatic effects (mean annual precipitation, and air temperature) on the spatial variability of the urban–rural phenological differences across cities. Monthly climate data of precipitation and temperature over 2007–2013 were obtained from Chinese Meteorological Observations (downloaded free from http://cdc.cma.gov.cn/). The meteorological station for each city was located in its urban area or nearby buffers (Zhou, Zhao, Liu, Zhang and Zhu, 2014). We assume that the data can reflect the overall climatic background for each city. Although urbanization may impact local climate to some extent, they should not alter the spatial pattern of the background climate significantly (Arnfield, 2003).

3. Results

The negative SOS differences (i.e., advance) and positive EOS differences (i.e., delay) averaged over the period 2007–2013 decayed exponentially and significantly ($p < 0.05$) with distance away from urban edge for over half of 32 cities (i.e., 21 for SOS and 17 for EOS). Insignificant trends were observed for most of the remaining cities, in particular for the southern cities of China (e.g., Guiyang, Guangzhou, and Shenzhen) (Fig. 4). For those cities with evident trends, the SOS and EOS differences were correlated negatively and positively ($p < 0.05$) with spring and autumn LST differences, respectively, in most cases (Table 1). On average, one degree increase of spring LST during the day and night resulted in an advance of the SOS by 11.4 ± 4.1 days (95% confidence intervals, hereafter) ($r = 0.91$, $p < 0.01$) and 8.7 ± 0.8 days ($r = 0.99$, $p < 0.01$), while one degree rise of autumn LST during day and night led to a delay of the EOS by 9.8 ± 3.7 days ($r = 0.91$, $p < 0.01$) and 5.6 ± 0.4 days ($r = 1.00$, $p < 0.01$), respectively (Fig. 5).

A great deal of spatial heterogeneities was indicated in urban–rural phenological differences across cities in China (Fig. 4). The SOS advanced in urban zones compared to rural areas in 27 out of 32 cites, with the SOS differences ranging from −27 days in Shenyang to

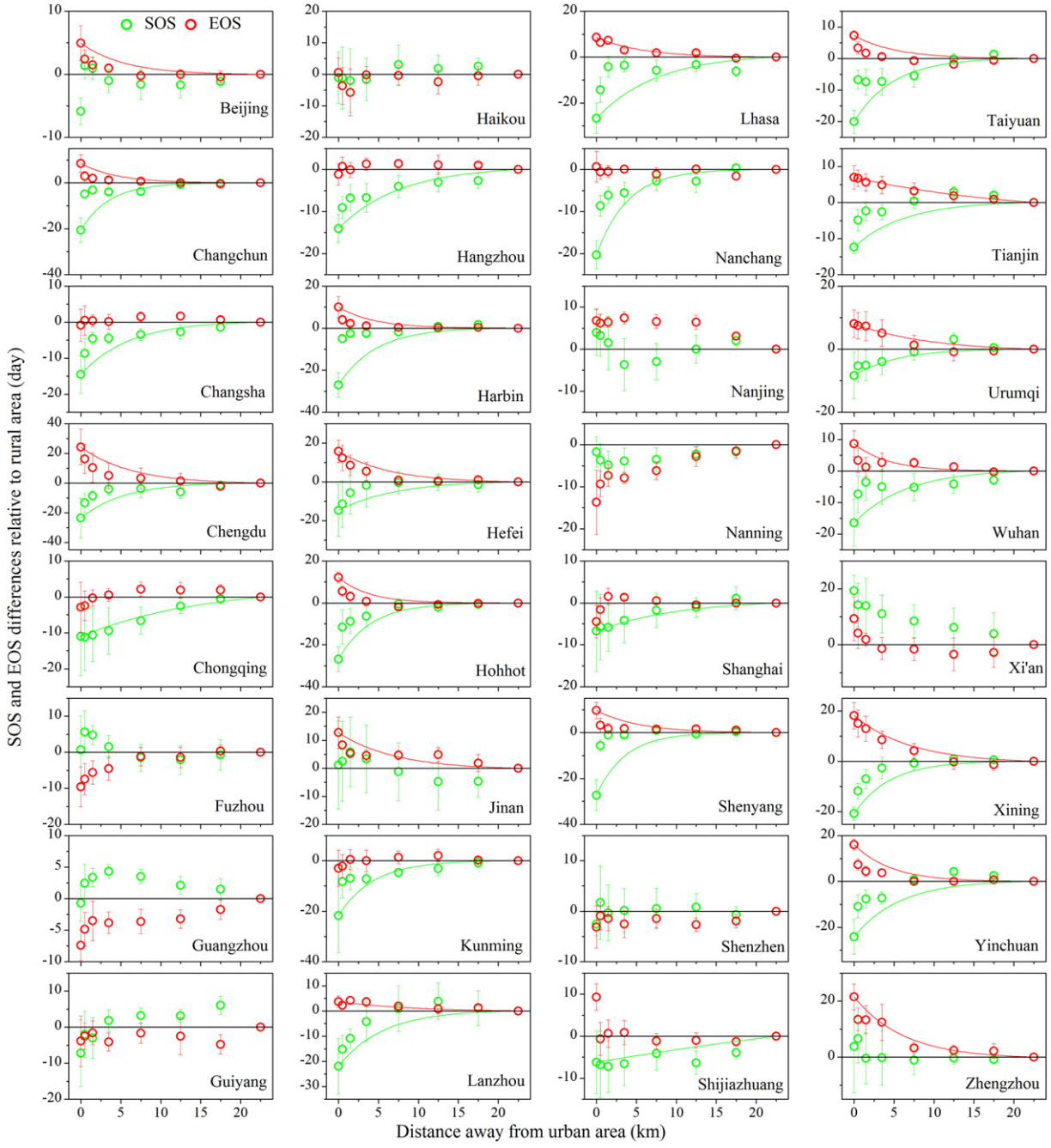

Fig. 4. Trends of the SOS and EOS differences relative to adjacent unaffected reference toward rural areas. The green and red lines represent the exponential fit curve of the SOS and EOS differences ($p < 0.05$) with distance away from urban areas, respectively. The error bars represent one standard deviation across years.

19 days in Xi'an. By contrast, EOS delayed in urban area in three-quarters of the cities, with the EOS differences ranging from 24 days in Chengdu to −14 days in Nanning. Consequently, the GSL was longer in urban than rural areas for majority of the cities (27 out of 32).

Overall, urbanization advanced the SOS in all the regions of China, with the largest of −25.0 (−27.2, −22.8) days (values in parentheses define the 95% confidence interval, hereafter) in Northeast China and the least of −4.7 (−9.6, 0.1) days in Central-south China (Fig. 6A). Comparatively, urbanization delayed the EOS in all the regions, although the delays were statistically insignificant over southeastern parts of China (i.e., East China, Central-south China, and Southwest China) (Fig. 6B). Northwest China and Central-south China witnessed the greatest [11.0 (6.6, 15.5) days] and least [0.8 (−6.9, 9.0) days] delays, respectively. On average, SOS advanced 11.9 (−15.7, −7.7) days and EOS delayed 5.4 (2.2, 8.6) days in the urban zones of the 32 cities relative to adjacent rural areas. As a result, the GSL was prolonged by 17.3 (11.6, 23.1) days (Fig. 6C).

4. Discussion

4.1. Trends of the urbanization effects on phenology of individual cities

Our results showed that the effect of urbanization on phenology was the greatest in urban centers and decreased exponentially toward rural areas for over half of the cities. The findings were generally in agreement with our hypothesis and the previous findings in the eastern North American (Zhang et al., 2004) and eastern China (Han & Xu, 2013). We further found that the advances of SOS or the delays of EOS

Table 1
Spearman's correlations between the phenological and land surface temperature differences relative to adjacent unaffected rural areas across urban and seven buffer areas. SOS and EOS represent the start and end of growing season, which were related to spring and autumn temperature differences, respectively.

City name	SOS		EOS		City name	SOS		EOS	
	Day	Night	Day	Night		Day	Night	Day	Night
Beijing	—	—	0.90[a]	0.76[b]	Lhasa	0.62	−0.69	0.60	0.93[a]
Changchun	0.21	−0.69	0.62	0.62	Nanchang	−0.50	−0.95[a]	—	—
Changsha	−0.76[b]	−0.38	—	—	Nanjing	—	—	—	—
Chengdu	−0.95[a]	−0.55	0.93[a]	0.93[a]	Nanning	—	—	—	—
Chongqing	−0.95[a]	−0.83[b]	—	—	Shanghai	−0.86[b]	−0.26	—	—
Fuzhou	—	—	—	—	Shenyang	−0.33	−0.83[b]	0.69	0.55
Guangzhou	—	—	—	—	Shenzhen	—	—	—	—
Guiyang	—	—	—	—	Shijiazhuang	0.00	−0.62	—	—
Haikou	—	—	—	—	Taiyuan	0.05	−0.90[a]	0.69	0.79[b]
Hangzhou	−0.60	−0.98[a]	—	—	Tianjin	0.74[b]	−0.93[a]	−0.19	0.98[a]
Harbin	−0.33	−0.90[a]	0.83[b]	0.90[a]	Urumqi	−0.24	−0.98[a]	−0.43	0.98[a]
Hefei	−1.00[a]	−0.24	0.62	0.40	Wuhan	−0.67	−0.48	0.81[b]	0.33
Hohhot	1.00[a]	−0.93[a]	−0.62	0.79[b]	Xi'an	—	—	—	—
Jinan	—	—	0.24	0.90[a]	Xining	−0.36	−0.98[a]	0.93[a]	0.88[a]
Kunming	−0.52	−0.98[a]	—	—	Yinchuan	−0.05	−0.67	0.33	0.45
Lanzhou	0.95[a]	−0.83[b]	−0.86[b]	0.79[b]	Zhengzhou	—	—	0.79[a]	0.93[b]

Day and night represent the relationships with daytime and nighttime land surface temperature differences, respectively.
"—", an insignificant trend of the phenological differences toward rural areas.
[a] Significant at 0.01 level.
[b] Significant at 0.05 level.

were linked closely with LST differences for most of those cities with evident phenological trends toward rural centers, characterized by a greater phenological change associated with a higher temperature difference. Similar phenomenon was reported by Zhang et al. (2004) in the eastern North American. This pattern was also highly consistent with the well-known temporal trends of the phenology associated with warming over northern mid-high latitudinal regions in recent decades (e.g., Cong et al., 2012; Jeong et al., 2011; Piao et al., 2006; White et al., 2009; Zeng et al., 2011).

Overall, we identified a strong phenological sensitivity to temperature for those cities with obvious phenological trends (Fig. 5), indicated by 9–11 days SOS advance and 6–10 days EOS delay per 1 °C increase of LST in spring and autumn, respectively. Zhang et al. (2004) reported 3-day SOS advance per 1 °C increase in LST in the eastern North America.

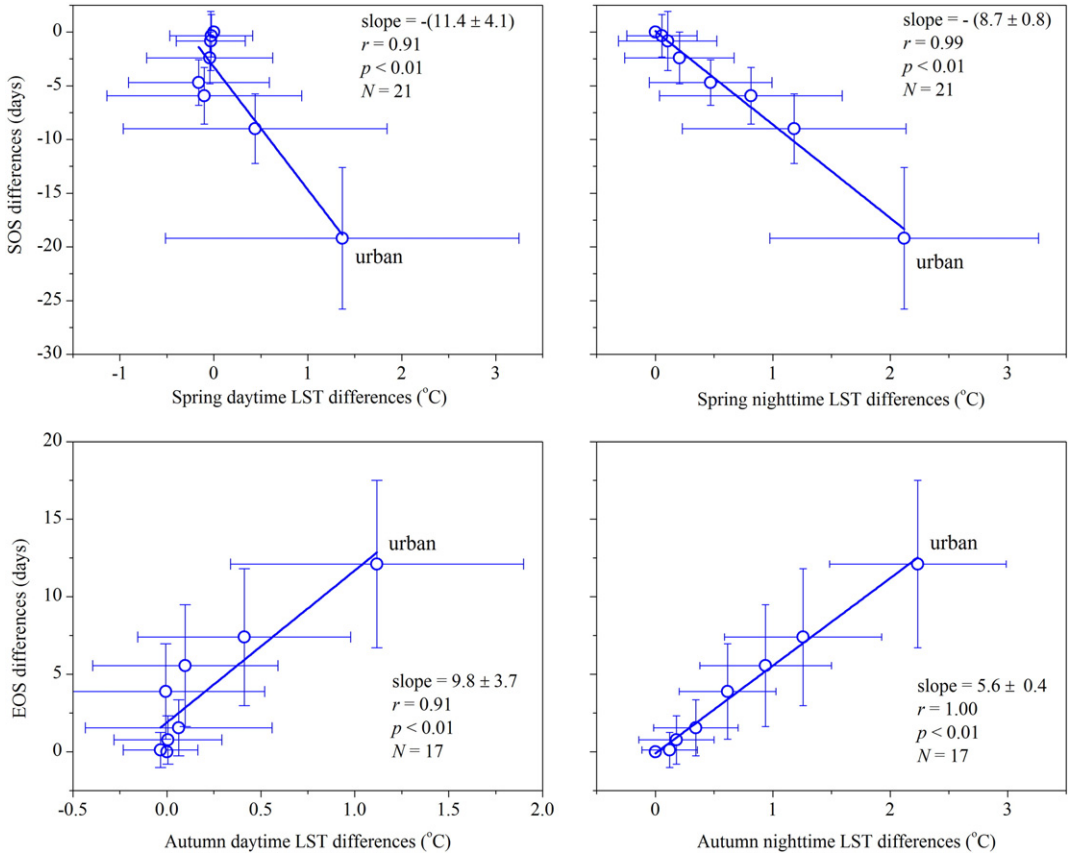

Fig. 5. linear regression slope (95% confidence intervals) between the SOS/EOS and land surface temperature (LST) differences (relative to rural areas) across urban and buffer (left to right, buffer 7 to 1) areas averaged over those cities that exhibited significant phenological trends ($p < 0.05$) toward rural areas. The error bar represents one standard deviation.

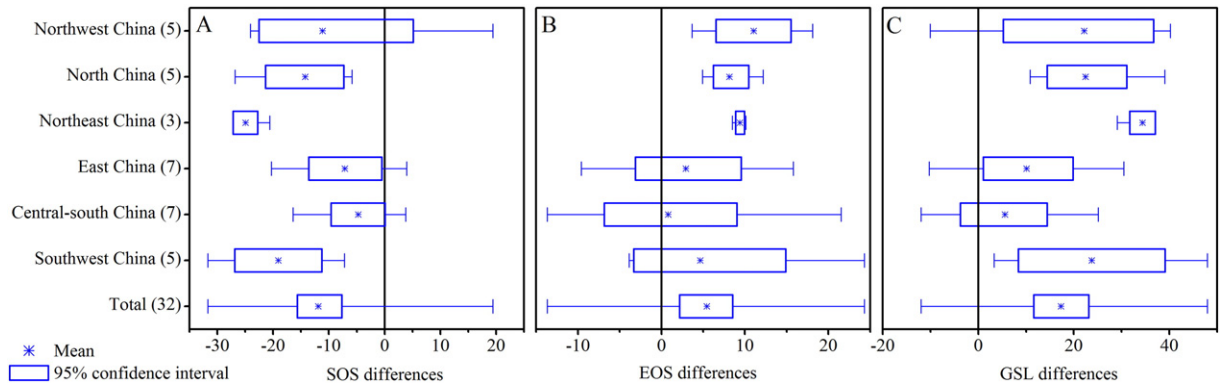

Fig. 6. The urban–rural differences of the SOS, EOS, and growing season length (GSL) in different geographic regions. The horizontal lower and upper error bars represent the minimum and maximum values, respectively.

The discrepancy might be attributed to the differences in research methods, study areas, study periods, and data sources (Cong et al., 2012; White et al., 2009).

4.2. Variations of the urbanization effects on phenology across cities

The urbanization effects on phenology varied across regions. The variability of the urbanization effects on phenology can be also identified by comparing the latitudinal trends of the phenological metrics between urban and rural areas (Fig. 7). The trends, in days per 1 °C latitude increase, of the urban SOS (0.75 ± 0.31, mean ± 1 standard error hereafter), EOS (0.23 ± 0.14), and GSL (−0.52 ± 0.42) were much weaker than those for their rural counterparts (1.32 ± 0.50), EOS (−0.56 ± 0.23), and GSL (−1.88 ± 0.59), respectively. These results also showed the increasing urbanization effects with increasing latitudes. This generally agrees with the recent global report by Peng et al. (2012) and our previous finding (Zhou, Zhao, Liu, Zhang and Zhu, 2014) that the urban heat island effects overall increase with latitudes.

The background climate strongly affects the geospatial variability of urbanization effects (Fig. 8). The magnitude of SOS advance and EOS delay (relative to rural zones) was negatively correlated with mean annual air temperature. This phenomenon can be attributed to the higher sensitivity of vegetation phenology to climate change in colder regions compared to warmer zones (Cong et al., 2012; Garonna et al., 2014; IPCC, 2013; Nemani et al., 2003). Moreover, the mean annual precipitation was also related to the urban–rural EOS difference (Fig. 8), consistent with previous observations (Cong et al., 2012; Jochner et al., 2013; Peñuelas et al., 2004; Zhang et al., 2004).

Our study showed that urban heat island (i.e., UHI) intensities were positively related to urban–rural SOS differences and negatively related to EOS differences across cities (Fig. 8), which is the opposite found by Zhang et al. (2004). The discrepancy might be caused by differences in (1) data and methods, and (2) background climate which is the ultimate factor that defines the spatial patterns of UHI effects across large geographical areas (Zhao et al., 2014; Zhou, Zhao, Liu, Zhang and Zhu, 2014). Global or cross-boundary studies should be conducted in the future to investigate the exact reasons for the difference.

Overall, the SOS advanced 11.9 (−15.7, −7.7) days and the EOS delayed 5.4 (2.2, 8.6) days in urban relative to adjacent rural areas for the 32 major Chinese cities. This phenomenon can be attributed to the fact that spring phenology is generally more sensitive to temperature than autumn phenology (White et al., 2002; Zhang et al., 2004). This pattern was consistent with the satellite observations in the eastern United States (White et al., 2002) and the field observations in the cities of Europe (Mimet et al., 2009; Roetzer et al., 2000) and China (Lu et al., 2006). Also, it agreed well with the well-known phenological trends through time over northern mid- to high-latitudes in response to global warming (e.g., Cong et al., 2012; Jeong et al., 2011; Piao et al., 2006; Zeng et al., 2011), further demonstrating the suitability of using urban areas as a natural laboratory to study phenological responses to global warming.

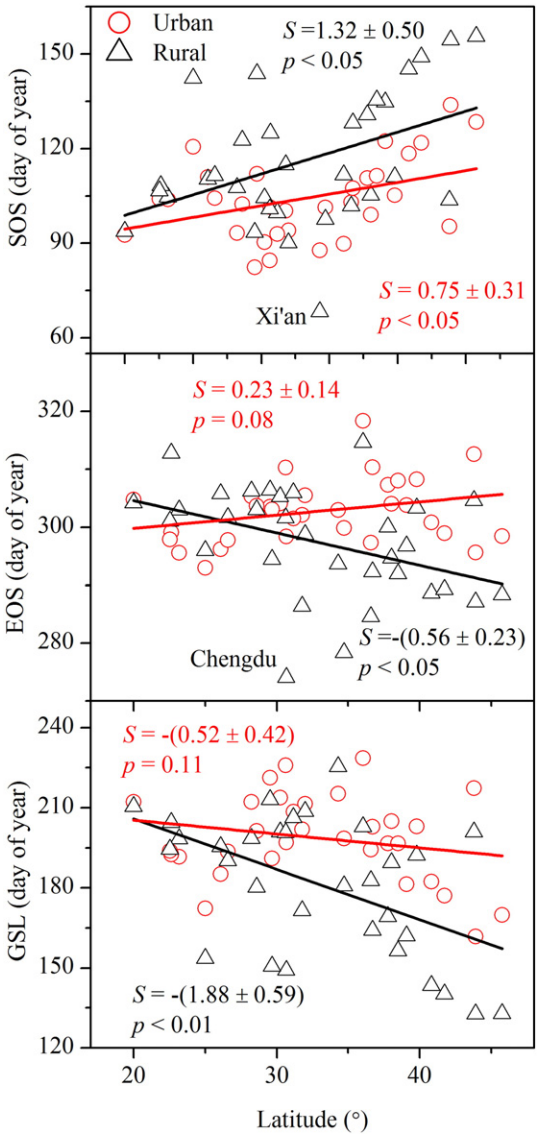

Fig. 7. Latitudinal trends of the SOS, EOS, and GSL in urban and rural areas for China's 32 major cities. *S* represents the linear slope. The bias-corrected bootstrapped standard error (based on 1000 bootstrap samples) was estimated for each slope.

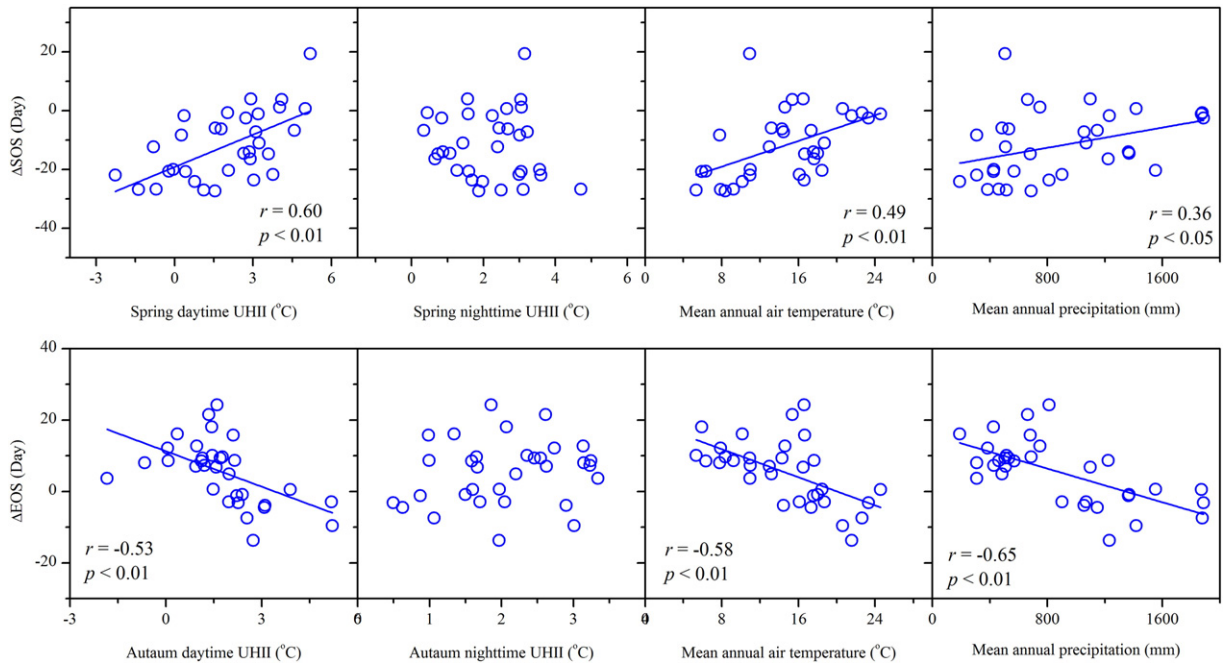

Fig. 8. Relationship between climatic factors or urban heat island intensity (UHII, urban–rural LST difference) and the urban–rural differences (△) of SOS/EOS across China's 32 major cities.

4.3. Uncertainties

Uncertainties existed in the results derived from this analysis. Several factors might contribute to those uncertainties. First, we did not exclude cropland from our study. The phenology of cropland depends strongly on crop type and human management and is generally characterized by faster greening and earlier harvesting (Buyantuyev & Wu, 2012; Zhang et al., 2004), resulting advances of SOS (i.e., Xi'an) and EOS (usually coupled with warming effect) in rural areas. The EVI in the rural areas of a few cities including Xi'an, Zhengzhou and Shijiazhuang presented two evident growing seasons per year because of double cropping (Fig. 9).

Second, in addition to temperature, other factors associated with urbanization such as species composition, hydrological regime, photoperiod, management practices (e.g., irrigation and nutrient application), and atmospheric environments (e.g., higher CO_2 concentrations) may influence the phenological activities (Buyantuyev & Wu, 2012; Gazal et al., 2008; Imhoff et al., 2004; Jach & Ceulemans, 1999; Jochner et al.,

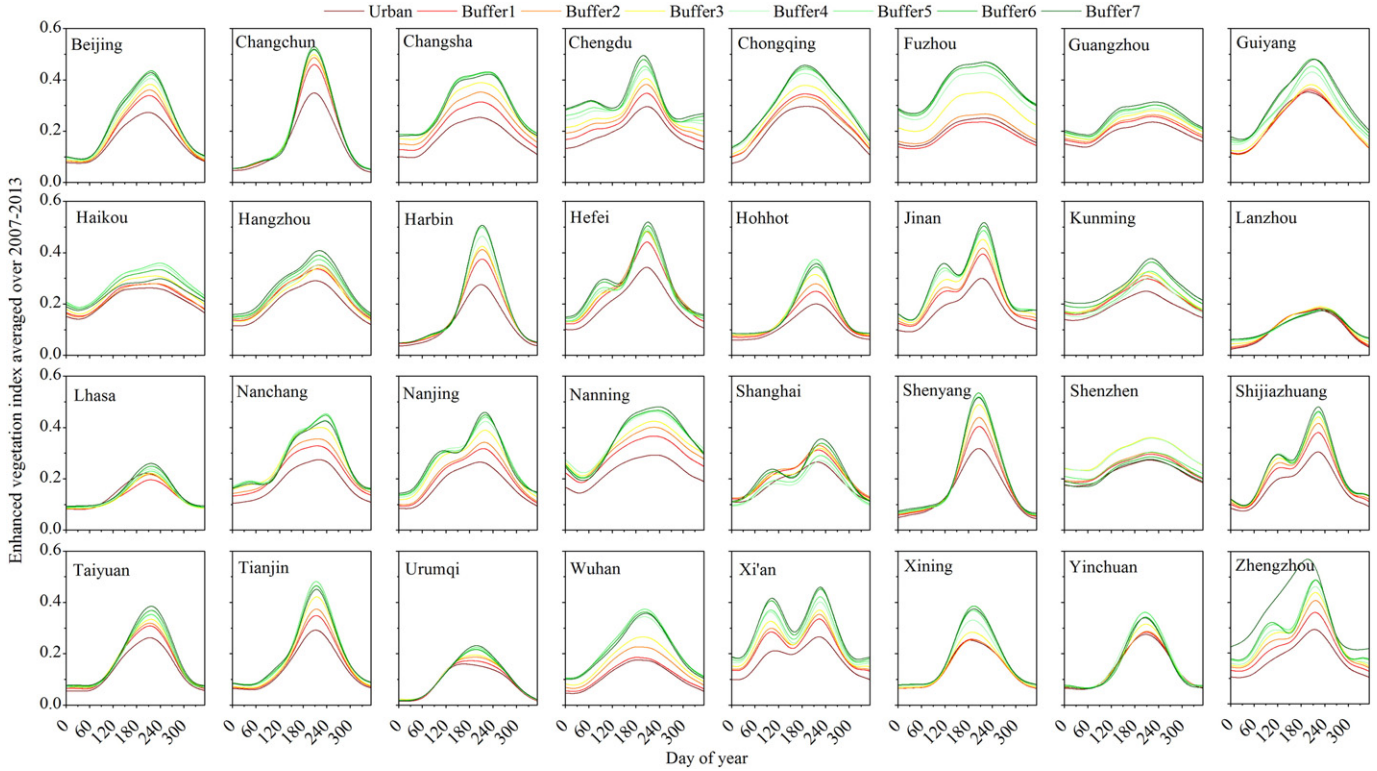

Fig. 9. Intra-annual variations of the smoothed enhanced vegetation index in urban areas and seven buffers (i.e., Buffer1 to Buffer7) for China's 32 major cities averaged over 2007–2013.

2013; Zhang et al., 2004). For example, urban vegetation frequently includes exotic species that may exhibit phenological patterns different from native plants. The urbanization effect on phenology may vary by species (Jochner et al., 2013), which might contribute to the large heterogeneity in phenology within a buffer or urban zone (Fig. 3). Moreover, urban vegetation is usually heavily managed, which may also affect the phenological patterns. Note that the number of cities with insignificant trends of the EOS (15 out of 32) was more than that of the SOS (11 out of 32), possibly indicating that other factors unconsidered play a more important role in controlling the EOS than the SOS, which was suggested by Zhang et al. (2004).

Third, data and methods may also introduce uncertainties. For example, there might be significant discrepancies between MODIS and ground-based vegetation index depending on climate conditions and geographic locations, especially for tropical regions (Hmimina et al., 2013). In particular, the seasonal patterns of the EVI for the tropical cities of China were not so evident (Fig. 9), because they are mainly covered by evergreen vegetation. This might contribute to the insignificant urbanization effects on phenology in many southern cities in China (Fig. 4). In addition, as mentioned above, there was double growing seasons per year for some cities because of the presence of double cropping (Fig. 9), and the double logistic algorithm we adopted might not perform very well in this situation (Atkinson, Jeganathan, Dash, & Atzberger, 2012). Moreover, we used the static land coverage maps in 2010 (Zhao et al., 2015) to delineate urban and buffer areas from 2007 to 2013. This would introduce some biases on the distribution of urban and buffer areas, especially for cities that experienced rapid urbanization, but should not change the phenological trends.

Our study focused mainly on the impacts of urbanization on land surface phenology using remotely sensed data. There is a clear need for continued phenological monitoring and research in urban areas in the future using both remote sensing technology and ground observations since urbanization-induced phenological shifts can exert strong impacts on both the eco-environments and human health (Neil & Wu, 2006) and can be used as natural laboratories to understand the impacts of future changes in climate (i.e., warming) and atmospheric composition (i.e., CO_2 concentration). While remote sensing is helpful in quantifying phenology at an ecosystem level, most issues mentioned above have to be addressed by direct observations and experimental manipulations.

Acknowledgments

This study was supported by the National Natural Science Foundation of China (#41571079, #41501465, and #31321061), the 111 Project (B14001), and the Startup Foundation for Introducing Talent of NUIST (2014r051). We thank Professor Ge Sun (Eastern Forest Environmental Threat Assessment Center, USDA Forest Service SouthernResearch Station), Professor Yongqiang Liu (Center for Forest Dis-turbance Science, USDA Forest Service Southern Research Station), and three anonymous reviewers for their valuable comments to improve this manuscript.

References

Angel, S., Parent, J., Civco, D.L., Blei, A., & Potere, D. (2011). The dimensions of global urban expansion: Estimates and projections for all countries, 2000–2050. *Progress in Planning*, *75*, 53–107.

Aono, Y., & Kazui, K. (2008). Phenological data series of cherry tree flowering in Kyoto, Japan, and its application to reconstruction of springtime temperatures since the 9th century. *International Journal of Climatology*, *28*, 905–914.

Arnfield, A.J. (2003). Two decades of urban climate research: A review of turbulence, exchanges of energy and water, and the urban heat island. *International Journal of Climatology*, *23*, 1–26.

Atkinson, P.M., Jeganathan, C., Dash, J., & Atzberger, C. (2012). Inter-comparison of four models for smoothing satellite sensor time-series data to estimate vegetation phenology. *Remote Sensing of Environment*, *123*, 400–417.

Baldocchi, D., Falge, E., Gu, L., Olson, R., Hollinger, D., Running, S., et al. (2001). FLUXNET: A new tool to study the temporal and spatial variability of ecosystem-scale carbon dioxide, water vapor, and energy flux densities. *Bulletin of the American Meteorological Society*, *82*, 2415–2434.

Brown, M.E., de Beurs, K., & Vrieling, A. (2010). The response of African land surface phenology to large scale climate oscillations. *Remote Sensing of Environment*, *114*, 2286–2296.

Buyantuyev, A., & Wu, J. (2012). Urbanization diversifies land surface phenology in arid environments: interactions among vegetation, climatic variation, and land use pattern in the Phoenix metropolitan region, USA. *Landscape and Urban Planning*, *105*, 149–159.

Cecchi, L., d'Amato, G., Ayres, J., Galan, C., Forastiere, F., Forsberg, B., Gerritsen, J., Nunes, C., Behrendt, H., & Akdis, C. (2010). Projections of the effects of climate change on allergic asthma: the contribution of aerobiology. *Allergy*, *65*, 1073–1081.

Chen, J., Jönsson, P., Tamura, M., Gu, Z., Matsushita, B., & Eklundh, L. (2004). A simple method for reconstructing a high-quality NDVI time-series data set based on the Savitzky–Golay filter. *Remote Sensing of Environment*, *91*, 332–344.

Clinton, N., & Gong, P. (2013). MODIS detected surface urban heat islands and sinks: Global locations and controls. *Remote Sensing of Environment*, *134*, 294–304.

Cong, N., Piao, S., Chen, A., Wang, X., Lin, X., Chen, S., et al. (2012). Spring vegetation green-up date in China inferred from SPOT NDVI data: A multiple model analysis. *Agricultural and Forest Meteorology*, *165*, 104–113.

Dallimer, M., Tang, Z., Bibby, P.R., Brindley, P., Gaston, K.J., & Davies, Z.G. (2011). Temporal changes in greenspace in a highly urbanized region. *Biology Letters*, *7*, 763–766.

Delbart, N., Picard, G., le Toan, T., Kergoat, L., Quegan, S., Woodward, I., et al. (2008). Spring phenology in boreal Eurasia over a nearly century time scale. *Global Change Biology*, *14*, 603–614.

Dragoni, D., & Rahman, A.F. (2012). Trends in fall phenology across the deciduous forests of the Eastern USA. *Agricultural and Forest Meteorology*, *157*, 96–105.

Eklundh, L., & Jönsson, P. (2009). *Timesat 3.0 software manual*. Sweden, Malmö and Lund: Lund University, 74.

Garonna, I., Jong, R., Wit, A.J., Mücher, C.A., Schmid, B., & Schaepman, M.E. (2014). Strong contribution of autumn phenology to changes in satellite-derived growing season length estimates across Europe (1982–2011). *Global Change Biology*, *20*, 3457–3470.

Gazal, R., White, M.A., Gillies, R., Rodemaker, E., Sparrow, E., & Gordon, L. (2008). GLOBE students, teachers, and scientists demonstrate variable differences between urban and rural leaf phenology. *Global Change Biology*, *14*, 1568–1580.

Han, G., & Xu, J. (2013). Land surface phenology and land surface temperature changes along an urban–rural Gradient in Yangtze River delta, China. *Environmental Management*, *52*, 234–249.

Hird, J.N., & McDermid, G.J. (2009). Noise reduction of NDVI time series: An empirical comparison of selected techniques. *Remote Sensing of Environment*, *113*, 248–258.

Hmimina, G., Dufrêne, E., Pontailler, J.Y., Delpierre, N., Aubinet, M., Caquet, B., et al. (2013). Evaluation of the potential of MODIS satellite data to predict vegetation phenology in different biomes: An investigation using ground-based NDVI measurements. *Remote Sensing of Environment*, *132*, 145–158.

Huete, A., Didan, K., Miura, T., Rodriguez, E.P., Gao, X., & Ferreira, L.G. (2002). Overview of the radiometric and biophysical performance of the MODIS vegetation indices. *Remote Sensing of Environment*, *83*, 195–213.

Imhoff, M.L., Bounoua, L., DeFries, R., Lawrence, W.T., Stutzer, D., Tucker, C.J., et al. (2004). The consequences of urban land transformation on net primary productivity in the United States. *Remote Sensing of Environment*, *89*, 434–443.

IPCC (2013). Summary for policymakers. In T.F. Stocker, D. Qin, G.K. Plattner, M. Tignor, S.K. Allen, J. Boschung, A. Nauels, Y. Xia, V. Bex, & P.M. Midgley (Eds.), *Climate change 2013: The physical science basis. Contribution of Working Group I to the fifth assessment report of the intergovernmental panel on climate change*. Cambridge, United Kingdom and New York, NY, USA: Cambridge University Press.

Jach, M.E., & Ceulemans, R. (1999). Effects of elevated atmospheric CO_2 on phenology, growth and crown structure of scots pine (*Pinus sylvestris*) seedlings after two years of exposure in the field. *Tree Physiology*, *19*, 289–300.

Jeong, S.J., Ho, C.H., Gim, H.J., & Brown, M.E. (2011). Phenology shifts at start vs. end of growing season in temperate vegetation over the northern hemisphere for the period 1982–2008. *Global Change Biology*, *17*, 2385–2399.

Jochner, S., Caffarra, A., & Menzel, A. (2013). Can spatial data substitute temporal data in phenological modelling? A survey using birch flowering. *Tree Physiology*, *33*, 1256–1268.

Jochner, S.C., Sparks, T.H., Estrella, N., & Menzel, A. (2012). The influence of altitude and urbanisation on trends and mean dates in phenology (1980–2009). *International Journal of Biometeorology*, *56*, 387–394.

Jönsson, P., & Eklundh, L. (2004). TIMESAT—a program for analyzing time-series of satellite sensor data. *Computers & Geosciences*, *30*, 833–845.

Keenan, T.F., Gray, J., Friedl, M.A., Toomey, M., Bohrer, G., Hollinger, D.Y., et al. (2014). Net carbon uptake has increased through warming-induced changes in temperate forest phenology. *Nature Climate Change*, *4*, 598–604.

Kramer, K. (1994). Selecting a model to predict the onset of growth of *Fagus sylvatica*. *Journal of Applied Ecology*, *31*, 172–181.

Kudo, G., Nishikawa, Y., Kasagi, T., & Kosuge, S. (2004). Does seed production of spring ephemerals decrease when spring comes early? *Ecological Research*, *19*, 255–259.

Liu, J., Liu, M., Tian, H., Zhuang, D., Zhang, Z., Zhang, W., et al. (2005). Spatial and temporal patterns of China's cropland during 1990–2000: An analysis based on Landsat TM data. *Remote Sensing of Environment*, *98*, 442–456.

Lu, P., Yu, Q., Liu, J., & Lee, X. (2006). Advance of tree-flowering dates in response to urban climate change. *Agricultural and Forest Meteorology*, *138*, 120–131.

Luo, Z., Sun, O.J., Ge, Q., Xu, W., & Zheng, J. (2007). Phenological responses of plants to climate change in an urban environment. *Ecological Research*, *22*, 507–514.

Mimet, A., Pellissier, V., Quénol, H., Aguejdad, R., Dubreuil, V., & Roze, F. (2009). Urbanisation induces early flowering: Evidence from *Platanus acerifolia* and *Prunus cerasus*. *International Journal of Biometeorology*, *53*, 287–298.

Neil, K., & Wu, J. (2006). Effects of urbanization on plant flowering phenology: A review. *Urban Ecosystems*, *9*, 243–257.
Nemani, R.R., Keeling, C.D., Hashimoto, H., Jolly, W.M., Piper, S.C., Tucker, C.J., et al. (2003). Climate-driven increases in global terrestrial net primary production from 1982 to 1999. *Science*, *300*, 1560–1563.
Oke, T. R. (1982). The energetic basis of the urban heat island. *Quarterly Journal of the Royal Meteorological Society*, *108*, 1–24.
Peng, S., Piao, S., Ciais, P., Friedlingstein, P., Ottle, C., Bréon, F.M., ... Myneni, R.B. (2012). Surface urban heat island across 419 global big cities. *Environmental Science & Technology*, *46*, 696–703.
Peñuelas, J., Filella, I., Zhang, X., Llorens, L., Ogaya, R., Lloret, F., et al. (2004). Complex spatiotemporal phenological shifts as a response to rainfall changes. *New Phytologist*, *161*, 837–846.
Piao, S., Ciais, P., Friedlingstein, P., Peylin, P., Reichstein, M., Luyssaert, S., et al. (2008). Net carbon dioxide losses of northern ecosystems in response to autumn warming. *Nature*, *451*, 49–52.
Piao, S., Fang, J., Zhou, L., Ciais, P., & Zhu, B. (2006). Variations in satellite-derived phenology in China's temperate vegetation. *Global Change Biology*, *12*, 672–685.
Piao, S., Fang, J., Zhou, L., Guo, Q., Henderson, M., Ji, W., ... Tao, S. (2003). Interannual variations of monthly and seasonal normalized difference vegetation index (NDVI) in China from 1982 to 1999. *Journal of Geophysical Research*, *108*, 4401.
Richardson, A.D., Black, T.A., Ciais, P., Delbart, N., Friedl, M.A., Gobron, N., et al. (2010). Influence of spring and autumn phenological transitions on forest ecosystem productivity. *Philosophical Transactions of the Royal Society, B: Biological Sciences*, *365*, 3227–3246.
Richardson, A.D., Keenan, T.F., Migliavacca, M., Ryu, Y., Sonnentag, O., & Toomey, M. (2013). Climate change, phenology, and phenological control of vegetation feedbacks to the climate system. *Agricultural and Forest Meteorology*, *169*, 156–173.
Rigo, G., Parlow, E., & Oesch, D. (2006). Validation of satellite observed thermal emission with in-situ measurements over an urban surface. *Remote Sensing of Environment*, *104*, 201–210.
Rodriguez-Galiano, V.F., Dash, J., & Atkinson, P.M. (2015). Intercomparison of satellite sensor land surface phenology and ground phenology in Europe. *Geophysical Research Letters*, *42*, 2253–2260.
Roetzer, T., Wittenzeller, M., Haechel, H., & Nekovar, J. (2000). Phenology in central Europe—Differences and trends of spring phenophases in urban and rural areas. *International Journal of Biometeorology*, *44*, 60–66.
Santandreu, M., & Lloret, F. (1999). Effect of flowering phenology and habitat on pollen limitation in Erica multiflora. *Canadian Journal of Botany*, *77*, 734–743.
Seto, K.C., Fragkias, M., Güneralp, B., & Reilly, M.K. (2011). A meta-analysis of global urban land expansion. *PloS One*, *6*, e23777.
Seto, K.C., Güneralp, B., & Hutyra, L.R. (2012). Global forecasts of urban expansion to 2030 and direct impacts on biodiversity and carbon pools. *Proceedings of the National Academy of Sciences of the United States of America*, *109*, 16083–16088.
United Nations (2014). *Department of Economic and Social Affairs, Population Division. World urbanization prospects: The 2014 revision*. New York: NY: United Nations.
van Vliet, A.J., Overeem, A., de Groot, R.S., Jacobs, A.F., & Spieksma, F. (2002). The influence of temperature and climate change on the timing of pollen release in the Netherlands. *International Journal of Climatology*, *22*, 1757–1767.
Wan, Z. (2008). New refinements and validation of the MODIS land-surface temperature/emissivity products. *Remote Sensing of Environment*, *112*, 59–74.
Wan, Z., & Dozier, J. (1996). A generalized split-window algorithm for retrieving land-surface temperature from space. *IEEE Transactions on Geoscience and Remote Sensing*, *34*, 892–905.
White, M.A., Beurs, D., Kirsten, M., Didan, K., Inouye, D.W., Richardson, A.D., et al. (2009). Intercomparison, interpretation, and assessment of spring phenology in North America estimated from remote sensing for 1982–2006. *Global Change Biology*, *15*, 2335–2359.
White, M.A., Nemani, R.R., Thornton, P.E., & Running, S.W. (2002). Satellite evidence of phenological differences between urbanized and rural areas of the eastern United States deciduous broadleaf forest. *Ecosystems*, *5*, 260–273.
Zeng, H., Jia, G., & Epstein, H. (2011). Recent changes in phenology over the northern high latitudes detected from multi-satellite data. *Environmental Research Letters*, *6*, 045508.
Zhang, X., Friedl, M.A., & Schaaf, C.B. (2006). Global vegetation phenology from moderate resolution imaging spectroradiometer (MODIS): Evaluation of global patterns and comparison with in situ measurements. *Journal of Geophysical Research*, *111*, G04017.
Zhang, X., Friedl, M.A., Schaaf, C.B., Strahler, A.H., & Schneider, A. (2004). The footprint of urban climates on vegetation phenology. *Geophysical Research Letters*, *31*, L12209.
Zhao, L., Lee, X., Smith, R.B., & Oleson, K. (2014). Strong contributions of local background climate to urban heat islands. *Nature*, *511*, 216–219.
Zhao, S., Zhou, D., Zhu, C., Qu, W., Zhao, J., Sun, Y., ... Liu, S. (2015). Rates and patterns of urban expansion in China's 32 major cities over the past three decades. *Landscape Ecology*. http://dx.doi.org/10.1007/s10980-015-0211-7.
Zhou, D., Zhao, S., Liu, S., & Zhang, L. (2014a). Spatiotemporal trends of terrestrial vegetation activity along the urban development intensity gradient in China's 32 major cities. *Science of the Total Environment*, *488*, 136–145.
Zhou, D., Zhao, S., Liu, S., Zhang, L., & Zhu, C. (2014b). Surface urban heat island in China's 32 major cities: Spatial patterns and drivers. *Remote Sensing of Environment*, *152*, 51–61.
Zhou, D., Zhao, S., Zhang, L., Sun, G., & Liu, Y. (2015). The footprint of urban heat island effect in China. *Scientific Reports*, *5*, 11160.
Ziska, L.H., Gebhard, D.E., Frenz, D.A., Faulkner, S., Singer, B.D., & Straka, J.G. (2003). Cities as harbingers of climate change: Common ragweed, urbanization, and public health. *Journal of Allergy and Clinical Immunology*, *111*, 290–295.